Formation of metastable iron carbide phases after high-fluence carbon ion implantation into iron at low temperatures

A. Königer, C. Hammerl, M. Zeitler, and B. Rauschenbach*
Institut für Physik, Universität Augsburg, D-86135 Augsburg, Germany
(Received 6 November 1996)

Carbon ions were implanted with an energy of 100 keV into thin iron layers at temperatures of −70 °C. Detailed analysis of structure was done by x-ray-diffraction synchrotron-radiation experiments. Phase formation was studied as a function of fluence from 1.2×10^{17} up to 1.2×10^{18} C^+/cm^2. The existence of cementite (θ-Fe_3C) and other metastable phases χ-Fe_5C_2 and η-Fe_2C is demonstrated and explained by lattice-invariant deformation. The sequence of phase transformation during subsequent annealing to temperatures of up to 450 °C was also investigated. The transformation sequence was found to end up in θ-Fe_3C, which is explained by a diffusion-determined process. [S0163-1829(97)04713-9]

I. INTRODUCTION

High-fluence ion implantation is an effective technique of forming metastable crystalline or amorphous phases, i.e., phases with a free energy higher than that of the stable phase under the prevailing conditions of temperature and pressure (e.g., see Refs. 1 and 2). The driving force for the implantation-induced formation and transformation of phases is provided by the ion energy loss during the penetration and subsequent stopping in the solid. If the temperature of the target is considerably lower than room temperature during implantation the effect of diffusion could be neglected. Only implantation-induced processes contribute to the phase formation. A significant number of experiments have demonstrated that metastable phases can be formed by implantation, but, at present, no general theory has been developed to predict which metastable phases can be expected.

The metal-nonmetal system iron/carbon is characterized by a solid solution (austenite, martensite), the well-known iron-cementite (θ-Fe_3C, cementite), and other metastable crystalline iron carbide phases (e.g., χ-Fe_5C_2 or Hägg-carbide, ϵ-Fe_2C_{1-x}).[3] From the thermodynamical point of view the iron carbide phases are very instable. The enthalpy of formation of Fe_2C and Fe_5C_2 is −2 kJ/mole and of Fe_3C is −1 kJ/mole, only.[4] According to Jack and Wild,[5] the exact phase identification in the Fe/C system is difficult because of the structural similarity of the carbide phases. The different iron carbide phases are summarized in Table I. In the case of high-fluence carbon ion implantation into iron previous work showed the formation of different stable and metastable crystalline iron carbide phases at room temperature or even higher temperatures.[9–11] Also hints for amorphization of iron by carbon ion implantation at room temperature could be found.[12] The formation of iron carbide phases at implantation temperatures considerably lower than room temperature is not proved.

In this paper we demonstrate the existence of metastable iron carbide phases after high-fluence carbon ion implantation at low temperatures in iron and the transformation of the formed metastable phases by subsequent annealing into a stable iron carbide phase. In this work by means of synchrotron radiation a highly precise tool was used to study the hardly detectable and distinguishable iron carbide diffraction spectra. The main advantages of synchrotron radiation is the very high intensity and high resolving power proved to be a well suited tool to study the Fe-C system.

II. EXPERIMENTAL CONDITIONS

Pure iron films with a thickness of 400 nm were deposited on (102) sapphire substrates by electron-beam evaporation with a rate of 0.1 ± 0.02 nm/s at a pressure of $>6\times10^{-6}$ mbar. Substrate temperature was held at 200 °C. Carbon ion implantation was performed at 100 keV with fluences ranging from 1.2×10^{17} C^+/cm^2 up to 1.2×10^{18} C^+/cm^2. Specimens were directly mounted on a liquid-nitrogen tank. Thus temperatures of about −70 °C at the target surface during implantation with ion-beam current densities of 6 ± 0.2 $\mu A/cm^2$ could be achieved. Temperature was controlled by a Ni-CrNi thermocouple which was clamped onto the sample surface. The iron films implanted with a fluence of 6×10^{17} C^+/cm^2 were annealed at temperatures of 150, 300, and 450 °C for 10 and 24 h, respectively. Annealing was performed in a vacuum furnace at a base pressure of 1×10^{-7} mbar (for details see Ref. 13). The x-ray-diffraction (XRD) experiments on thin implanted iron films were performed at the synchrotron-radiation source in Hamburg (HASYLAB of the DESY Hamburg) with monochromatic radiation (wavelength $\lambda=0.13$ nm). Only the diffraction spectra between $2\theta=30°$ and 42° are presented, because the strongest peaks of the expected iron carbide phases are located within this range. All diffraction measurements were carried out at room temperature. Composition was investigated using Rutherford backscattering spectroscopy (RBS). 2.5 MeV He^{2+} ions served as projectiles which were detected under an angle of 170°.

III. RESULTS AND DISCUSSION

RBS spectra of Fe layers on Si before implantation and after implantation with different carbon ion fluences at −70 °C are presented in Fig. 1(a). After implantation the dip in the Fe signal comes from a near Gaussian distribution of

TABLE I. Lattice parameters, carbon concentration, and crystallographical data of the iron carbide phases and solid solutions (Refs. 3 and 6–8).

Phase	Composition	Carbon concentration (at. %)	Bravais lattice	Lattice parameters (nm) (at RT)
Iron	α-Fe		bcc	$a=0.28663$
Austenite		0 . . . 8.3	fcc	$a=0.3572+0.00078$ (at. % C)
Martensite	α'-Fe(C)	0 . . . 8.3	bct	$a=0.28664-0.00028$ (at. % C)
				$c/a=1+0.0096$ (at. % C)
Cementite	θ-Fe_3C	25.0	Orthorh.	$a=0.45248$
				$b=0.50896$
				$c=0.67443$
Hagg-carbide	χ-Fe_5C_2	28.6	Monocline	$a=1.1562$
				$b=0.4573$
				$c=0.5060$
				$\beta=97.74°$
ϵ-carbide	ϵ-Fe_2C_{1-x}	29.4 (at $Fe_{2.4}C$)	Hex.	$a=0.2754$
				$c=0.43486$ (at $Fe_{2.4}C$)
η-carbide	η-Fe_2C	33.0	Orthorh.	$a=0.4704$
				$b=0.4318$
				$c=0.2830$

carbon centered around the projected range. In the case of implantation with 100 keV carbon ions in iron the mean projected range is about 150 nm. The corresponding carbon ion range profile is plotted in Fig. 2(a). A specially designed computer code was used to convert the spectra from Fig. 1 into concentration profiles (see Fig. 2). For the implanted fluences from 1.2×10^{17} C^+/cm^2 up to 1.2×10^{18} C^+/cm^2 the maximum carbon ion concentration varies from 10 at. % carbon up to 65 at. % carbon. It has to be noted that these concentrations are far above the mean concentrations necessary to reach stoichiometric conditions of any iron carbide[8] (see also Table I). Figures 1(b) and 2(b) show the RBS spectra of iron implanted with 6×10^{17} C^+/cm^2 before annealing (as implanted) and after subsequent annealing at different temperatures for 10 or 24 h, respectively. Significant differences between the as implanted state and that after annealing can be observed. Annealing for 24 h at 150 °C leads to a decrease from 45 at. % carbon to about 40 at. % carbon of the concentration at the peak maximum. Annealing at 300 °C for 10 h leads to an evident broadening of the carbon profile. The concentration maximum is decreased down to 32 at. % carbon. If higher temperatures (450 °C, 10 h) are chosen further flattening of the profile takes place. The stoichiometric concentration of 25 at. % carbon for Fe_3C is reached.

Figure 3 shows XRD spectra of iron after implantation with carbon ions at a temperature of −70 °C as a function of the carbon ion fluence ranged from 1.2×10^{17} up to 1.2×10^{18} C^+/cm^2. Only the spectra between $2\theta=30°$ and 42° are presented. The RBS measurements have demonstrated that these

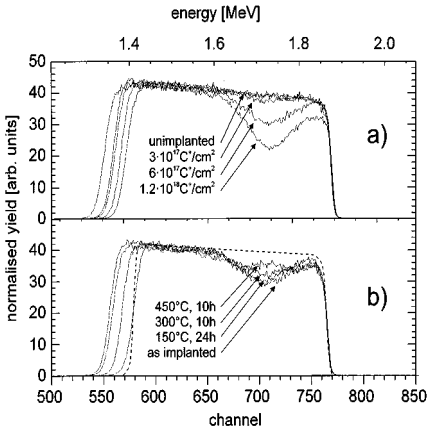

FIG. 1. Rutherford backscattering spectra of (a) iron implanted with 100 keV carbon ions at −70 °C with different fluences and (b) iron implanted with 6×10^{17} C^+/cm^2 at 100 keV as implanted ($T_i=-70$ °C) and annealed (150 °C/24 h, 300 °C/10 h, 450 °C/10 h). Simulation of pure iron sample (dotted line) as a guide to the eye.

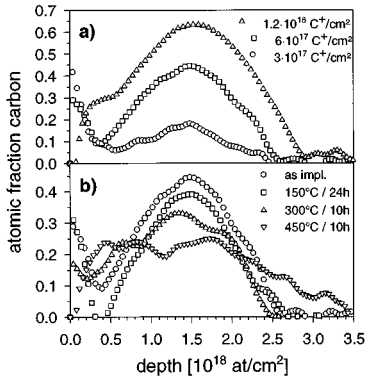

FIG. 2. Carbon concentration profiles extracted from RBS spectra (see Fig. 1). Showing the variation of (a) fluence (from 6×10^{17} C^+/cm^2 up to 6×10^{17} C^+/cm^2) and (b) annealing conditions [as implanted ($T_i=-70$ °C) and annealed (150 °C/24 h, 300 °C/10 h, 450 °C/10 h)] for 100 keV carbon ion implantation into iron.

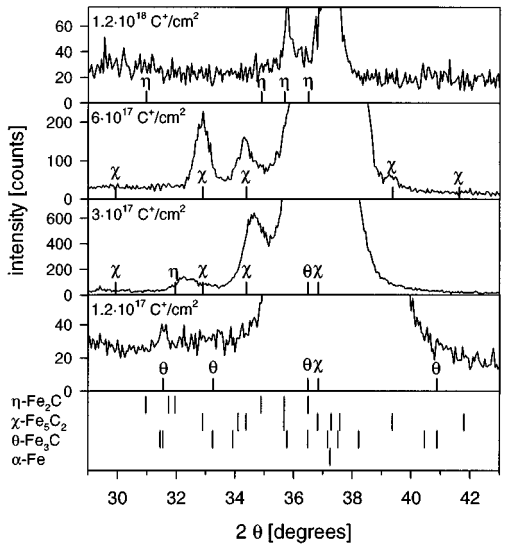

FIG. 3. XRD spectra of iron implanted with 100 keV carbon ions at −70 °C. Fluences ranging from 1.2×10^{17} C^+/cm^2 up to 1.2×10^{18} C^+/cm^2. Most intense reflections for iron carbide phases are indicated below. Note the choice of the intensity axis in the different spectra.

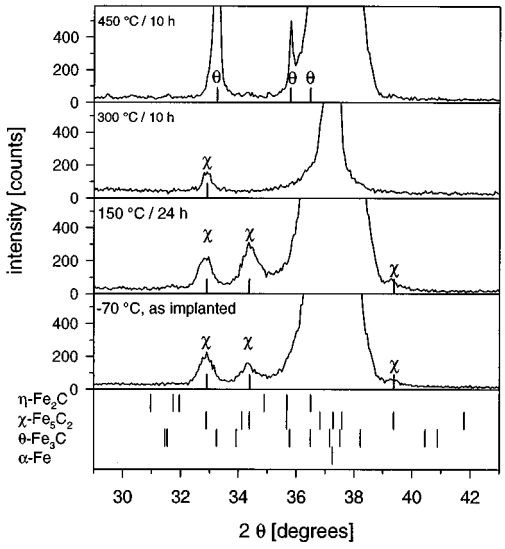

FIG. 4. XRD spectra iron after implantation with 6×10^{17} C^+/cm^2 at −70 °C and after annealing at 150 °C for 24 h, at 300 °C for 10 h and 450 °C for 10 h, respectively.

fluences correspond to concentrations between 10 and 65 at. % carbon. All samples exhibit a very strong peak at $2\theta=37.25°$ referring to the α-Fe (110) reflection. The derivation of the experimentally determined interplanar spacing d_{exp} from the theoretically expected interplanar spacing $d_{theo}=0.20268$ nm was always $<0.08\%$. In addition to the (110) α-Fe diffraction peak weak reflections especially at $2\theta=31.55°$ and 41.09° are found after implantation with the lowest fluence of 1.2×10^{17} C^+/cm^2. These can be correlated with the θ-Fe_3C (210) and (221) peaks of the stable iron-cementite phase, only (see Table II). With increase of the carbon ion fluence to 3×10^{17} C^+/cm^2 reflections of iron-cementite and also of the metastable Hägg carbide, χ-Fe_5C_2, could be detected. The intensities of these XRD reflections are increased, i.e., the volume fraction of these iron carbide phases is higher with increasing carbon ion fluences. Implantation of 6×10^{17} C^+/cm^2 results in further formation of the metastable iron carbide phase, χ-Fe_5C_2. The reflections of this phase can clearly be separated from others by several strong peaks. Diffraction data supplies reflections at $2\theta=32.83°$, 34.33°, and 39.28° which arise from χ-Fe_5C_2 (020), (112), and (221) planes (see Table II). These peaks disappear after implantation of 1.2×10^{18} C^+/cm^2. Small but distinct peaks arise at $2\theta=34.85°$, 35.75°, and 47.35° indicating the presence of the iron carbide phase η-Fe_2C. The structure of the orthorhombic η-carbide is very similar to the structure of the hexagonal iron carbide phase ϵ-Fe_2C_{1-x} (lattice parameters: $a_\eta\approx\sqrt{3}a_\epsilon$, $b_\eta\approx c_\epsilon$, $c_\eta\approx a_\epsilon$).[8] The major difference between both structures is the arrangement of the carbon atoms. In contrast to the ϵ-carbide, in the η-carbide the carbon atoms produce a sublattice by regularly filling one-half of the octahedral sites between the iron atoms. Consequently, the reflection of the η-phase cannot be distinguished from the ϵ-phase within the experimental constraints for thin films. It can be summarized that with the increase of the carbon ion fluence from 1.2×10^{17} up to 1.2×10^{18} C^+/cm^2, i.e., with the increasing of the carbon content in iron from 10 at. % up to 65 at. % carbon, more and more rich-carbon phases from θ-Fe_3C (25 at. % C) through χ-Fe_5C_2 (28.6 at. %) to η-Fe_2C (33 at. %) are formed. The formation of these phases is a result of the implantation. The diffusivity of carbon in iron is very low ($<10^{-20}$ cm^2/s) and the iron self-diffusion is almost negligible at the implantation temperature of −70 °C.[7] Therefore, the phase formation should be explained in the context of the implantation, i.e., in the absence of long-range diffusion.

Two types of interstices are available in the iron system taking into account all allotropic modifications of this system. But carbon atoms only occupy the octahedral sites, never the tetrahedral ones. In the very early stages of carbon ion implantation carbon occupies those sites. By introducing more and more carbon atoms a large anisotropic strain is built up. Hence the solubility of interstitial atoms is very small. Carbon contents exceeding the equilibrium solubility lead to an arrangement of prisms where there is localized distortion to accommodate a carbon atom. Iron-cementite is an example for an arrangement of such trigonal prisms.[14] Further increase in the number of incorporated carbon atoms would require pronounced distortion and results in the formation of metastable χ-Fe_5C_2, first, and then in the formation of the η-Fe_2C phase. The structure of both metastable phases has again been described on the basis of the arrangement of trigonal prisms.[7] The positions of the carbon atom within one prism and the arrangement of the prisms is slightly changed in these phases. The sequence of phase transformation of iron carbide phases by annealing is presented in Fig. 4. As described above in the as implanted state after implantation 6×10^{17} C^+/cm^2 at −70 °C the existence of χ-Fe_5C_2 is evident. Strong reflections at $2\theta=32.83°$, 34.33°, and 39.28° are detected. Annealing at 150 °C for 24 h leads to an enhancement of the intensities of these peaks. If a temperature of 300 °C is provided for 10 h the intensity of these peaks is strongly reduced. Only the reflection at $2\theta=32.83°$ corresponding to (020) χ-Fe_5C_2 is visible. Addi-

TABLE II. Comparison of the experimentally determined interplanar spacings d_{exp} with the theoretically determined interplanar spacings d_{theo} within the 2θ range from 30° up to 48° of iron after carbon ion implantation at −70 °C with different fluences. The derivation between d_{exp} and d_{theo} is given by $\Delta d = |d_{theo} - d_{exp}|/d_{theo}$. 100% and hkl are the Miller indices.

	Experiment		Theory			
Fluence	2θ	d_{exp} (nm)	d_{theo} (nm)	Δd (%)	(hkl)	Phase
1.2×10^{17} C^+/cm^2	31.55	0.238 10	0.238 15	0.02	(210)	θ-Fe_3C
	33.14	0.226 97	0.226 31	0.29	(002)	θ-Fe_3C
	36.73	0.205 45	0.206 78	0.64	(102)	θ-Fe_3C
		0.205 45	0.204 93	0.25	(510)	χ-Fe_5C_2
	41.09	0.184 45	0.185 34	0.48	(221)	θ-Fe_3C
3×10^{17} C^+/cm^2	29.42	0.254 92	0.250 63	1.71	(002)	χ-Fe_5C_2
	32.31	0.232 64	0.235 20	1.09	(200)	η-Fe_2C
	33.04	0.227 64	0.228 65	0.44	(020)	χ-Fe_5C_2
	34.64	0.217 43	0.219 06	0.75	(202)	χ-Fe_5C_2
	36.73	0.205 45	0.206 78	0.64	(102)	θ-Fe_3C
		0.205 45	0.204 93	0.25	(510)	χ-Fe_5C_2
6×10^{17} C^+/cm^2	29.67	0.252 82	0.250 63	0.87	(002)	χ-Fe_5C_2
	32.83	0.229 06	0.228 65	0.18	(020)	χ-Fe_5C_2
	34.33	0.219 33	0.219 06	0.12	(202)	χ-Fe_5C_2
	39.28	0.192 59	0.192 17	0.22	(221)	χ-Fe_5C_2
	41.87	0.181 16	0.182 16	0.55	(511)	χ-Fe_5C_2
1.2×10^{18} C^+/cm^2	30.95	0.242 60	0.242 50	0.04	(101)	η-Fe_2C
	34.85	0.216 16	0.215 90	0.12	(020)	η-Fe_2C
	35.75	0.210 89	0.211 30	0.20	(111)	η-Fe_2C
	36.75	0.205 34	0.206 70	0.66	(210)	η-Fe_2C
	47.35	0.161 20	0.161 20	0.00	(121)	η-Fe_2C

tionally it has to be noticed that the (110) Fe peak at $2\theta = 37.25°$ is sharper. Annealing at even higher temperatures (450 °C for 10 h) leads to completely different diffraction spectra. The previous peak at $2\theta = 32.83°$ has disappeared and another one with high intensity arises at $2\theta = 33.25°$. This peak can be identified with the (002) reflection of θ-Fe_3C. Additional reflections observed at $2\theta = 69.80°$ and 72.68° which can clearly be identified with (152) and (430) θ-Fe_3C reflections, confirm the existence of the θ-Fe_3C phase.

Thus it can be concluded that χ-Fe_5C_2 iron carbide existing after implantation enlarges its volume portion after annealing at 150 °C. At 300 °C this phase starts to transform to the stable θ-Fe_3C, which is the dominant phase after annealing at 450 °C. The sequence of phase transformation from the metastable χ-Fe_5C_2 phase, rich in carbon, to the stable iron-cementite with a lower carbon content has been observed. It should be noted that for higher carbon fluences the formed η-Fe_2C (ϵ-Fe_2C_{1-x}) is first transformed to χ-Fe_5C_2 and then, in a second stage, to the stable θ-Fe_3C phase. The iron-cementite and the Hägg-carbide have close similarities between the structures ($a_\theta \approx b_\chi$, $b_\theta \approx c_\chi$, $2c_\theta \approx a_\chi$).[7] The carbon atom environment in both phases is a trigonal prism of iron atoms. These prisms are joined together by sharing edges and corners. In the θ-Fe_3C phase the prisms form sheets which are stacked perpendicular to the c axis, whereas in the case of χ-Fe_5C_2 iron carbide the prisms form double sheets in the monoclinic (100) plane. The decomposition of the Hägg-carbide χ-Fe_5C_2 to iron cementite is determined by a diffusion-controlled process. The carbon atoms in the trigonal prisms are able to diffuse away during annealing at higher temperatures. This process results in a reduction of the localized distortion and an atomic arrangement of carbon and iron, the cementite phase.[14] This thermodynamically induced phase transition leads to an orthorhombic, more closely packed structure.

IV. SUMMARY

In conclusion the phase formation of iron carbide phases after ion implantation at low temperatures (−70 °C) was studied. With increasing ion fluences the existence of θ-Fe_3C, χ-Fe_5C_2, and also η-Fe_2C for the highest fluences was proved. Besides phase formation during ion implantation phase transformation during subsequent annealing was also studied by means of XRD synchrotron-radiation experiments. The transformation sequence χ-$Fe_5C_2 \rightarrow \theta$-$Fe_3C$ during annealing was confirmed. The transformation of the different iron carbide phases can be explained by a diffusion-determined process.

ACKNOWLEDGMENTS

The authors thank Dr. S. Doyle and Dr. T. Wroblewski (HASYLAB Hamburg) for assistance during diffraction measurements.

*Author to whom correspondence should be addressed: Bernd Rauschenbach, Universität Augsburg, Institut für Physik, Memminger Strasse 6, D-86135 Augsburg, Germany. FAX: +49 821 598 3425. Electronic address: rauschen@physik.uni-augsburg.de

[1] N. Nastasi and J. W. Mayer, Mater. Sci. Rep. **6**, 1 (1991).
[2] G. S. Was, Prog. Surf. Sci. **32**, 211 (1989).
[3] J. Kunze, *Nitrogen and Carbon in Iron and Steel* (Akademie-Verlag, Berlin, 1990).
[4] F. R. deBoer, R. Boom, W. C. M. Mattens, A. R. Miedema, and A. K. Niessen, *Cohesion in Metals* (North-Holland, Amsterdam, 1988), Vol. 1, p. 231.
[5] K. H. Jack and S. Wild, Nature (London) **212**, 248 (1966).
[6] R. C. Ruhl and M. Cohen, Trans. AIME **245**, 241 (1969).
[7] D. L. Williamson, K. Nakazawa, and G. Krauss, Metall. Trans. **10A**, 1351 (1979).
[8] D. H. Jack and K. H. Jack, Mater. Sci. Eng. **11**, 1 (1973).
[9] D. M. Follstaedt, Nucl. Instrum. Methods Phys. Res. Sect. B **7/8**, 11 (1985).
[10] A. M. C. Pérez, A. M. Vredenberg, L. de Wit, J. S. Custer, Mater. Sci. Eng. B **19**, 281 (1983).
[11] A. Sekiguchi, T. Fujihana, M. Yuasa, I. Sekine, K. Akashi, K. Takahashi, M. Iwaki, Surf. Coat. Technol. **51**, 13 (1992).
[12] D. M. Follstaedt and J. A. Knapp, EMRS Proc. **51**, 473 (1986).
[13] A. Königer, A. Wenzel, C. Hammerl, W. Zander, B. Rauschenbach, and B. Stritzker, Rev. Sci. Instrum. **67**, 3961 (1996).
[14] E. J. Fasiska and G. A. Jeffrey, Acta Crystallogr. **19**, 463 (1965).